Tunable self-organization of nanocomposite multilayers

Chen, C.Q.; Pei, Y. T.; Shaha, K. P.; de Hosson, J. Th. M.

Published in:
Applied Physics Letters

DOI:
10.1063/1.3318262

Publication date:
2010

Tunable self-organization of nanocomposite multilayers

C. Q. Chen, Y. T. Pei, K. P. Shaha, and J. Th. M. De Hosson[a)]
Department of Applied Physics, Materials Innovation Institute (M2i), University of Groningen, Nijenborgh 4, 9747 AG Groningen, The Netherlands

(Received 25 December 2009; accepted 18 January 2010; published online 16 February 2010)

In this letter we report the controlled growth and microstructural evolution of self-assembled nanocomposite multilayers that are induced by surface ion-impingement. The nanoscale structures together with chemical composition, especially at the growing front, have been investigated with high-resolution transmission electron microscopy. Concurrent ion impingement of growing films produces an amorphous capping layer 3 nm in thickness where spatially modulated phase separation is initiated. It is shown that the modulation of multilayers as controlled by the self-organization of nanocrystallites below the capping layer, can be tuned through the entire film. © *2010 American Institute of Physics*. [doi:10.1063/1.3318262]

Recently self-assembling has been realized and utilized in the growth of thin films with nanoscale ordered structures, like superlattices or multilayers in metal-metal[1,2] and metal-carbon systems.[3–7] Despite the experimental accomplishments, understanding of the physical mechanism and the driving force is still rather limited, partially due to the fact that a high spatial resolution examination of the structures were not performed. Self-assembling is often associated with surface irradiation,[2,6,7] high temperature,[7] metal species and content,[5,7] deposition rate,[4] etc. However, the atomic underpinning mechanism is still rather obscure. Also, the self-organized nanocomposite multilayers reported in literature generally degrade fast and the modulation is lost after growth of tens of nanometers.[3–7] Further, the driving force of self-organization, i.e., whether it refers to nucleation and growth or spinodal decomposition, is still under debate.[5,7]

In this letter, we present tunable and sustainable growth of self-organized nanocomposite multilayers by surface ion-impingement during sputter deposition of carbon and Ti. The evolution of the nanostructure with growth (thickness) is investigated in detail by combined atomic scale high resolution cross-sectional transmission electron microscopy (HR-XTEM) and energy filtered XTEM.

TiC/amorphous carbon (a-C) nanocomposite films were deposited on Si wafer by nonreactive pulse-dc (p-dc) magnetron sputtering of Ti and graphite targets, with a TiCr interlayer to improve the adhesion. The details of the experimental setup are referred to our recent work.[8] The metal targets were powered by a double channel dc power supply while the graphite targets were powered by a p-dc power supply. The substrate was also biased by p-dc. The substrate was rotated at 3 rpm during deposition. Structure characterization was performed in a JEOL 2010FEG high resolution TEM operating at 200 kV and having a Gatan energy filtering system.

The deposition and structural parameters of the TiC/a-C nanocomposite films studied are listed in Table I. The films are termed by a combination of pulse frequency and substrate bias voltage. With increasing the p-dc frequency, the sputtering yield of graphite targets decreases so that the content of carbon in the films is getting lower even though the sputtering current applied to the targets were kept unchanged for the first three films. On the other hand, increasing substrate bias voltage enhances the resputtering of carbon atoms from a deposited film, also leading to the reduction of carbon content. Accordingly, the composition of the nanocomposite films covers a wide range of interest. The XTEM of the nanostructures of the films is shown in Fig. 1. The film deposited at 100 kHz shows a homogeneous nanocomposite structure with weak contrast of crystalline domains; while those deposited at pulse frequencies higher than 250 kHz posses multilayered structures, with tunable bilayer thickness that increases with increasing p-dc frequency and substrate bias voltage. The multilayers are composed of alternating Ti-rich and C-rich layers, with the darker ones containing aligned TiC nanocrystallites separated by a-C boundaries,

TABLE I. Chemical composition of TiC/a-C films, size d of TiC NCs, wavelength Λ of the multilayers, revolutions n needed to yield a bilayer, surface roughness w, and impingement enhanced diffusion coefficient $\bar{D}^*$. Sputtering currents applied to Ti and graphite targets are $I_{Ti}=0.35$ A and $I_C=1.5$ A, respectively, except $I_{Ti}=0.55$ A for the last film for comparison.

Film code	Composition (at. %)			Λ (nm)	d (nm)	n	w (nm)	$\bar{D}^*$ ($\times 10^{-19}$ m^2 s^{-1})
	C	Ti	O					
100k40V	89.8	9.7	0.5	Homogeneous	~2		4.6	
250k40V	86.6	12.9	0.5	6.7	3–5	3.7	0.3	−1.5
350k40V	80.1	19.3	0.6	9.8	4–6	6	0.28	−2.0
350k100V	75.2	23.9	0.9	14.2	3–7	11	0.23	−2.3
350k40V0.55	66.3	32.7	1.0	Weak multilayer	3–7		0.25	

[a)]Author to whom correspondence should be addressed. Electronic mail: j.t.m.de.hosson@rug.nl. Tel.: +31-50-363 4898. FAX: +31-50-363 4881.

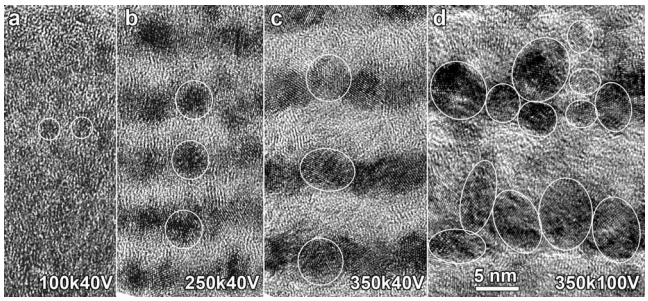

FIG. 1. HR-XTEM images showing the structure evolution of p-dc deposited TiC/a-C film with increasing pulse frequency and substrate bias. Circles in white color mark TiC NCs.

while the bright ones being C-rich layer mainly composed of a-C.

From a closer examination of the nanostructures it turns out that the formation of these multilayers is a spontaneously assembling process via phase separation, rather than a direct result of the sequential deposition of Ti and C species, as the formation of a bilayer generally involves more than one substrate revolutions, e.g., 3.7, 6, and 11 revolutions for the films 250k40V, 350k40V, and 350k100V, respectively. Obviously, the number of revolutions yielding one bilayer increases with increasing pulse frequency and/or substrate bias voltage. Consequently, the bilayer thickness of the three films equals to 6.7, 9.8, and 14.2 nm, respectively, despite the slight decrease of deposition rate. Presumably this trend is associated with the intensified concurrent Ar ions impingement at the growing surface at higher pulse frequency and substrate bias voltage.[8] A detailed evaluation of the energy distribution of impinging ions shows that the energy flux coincides well with the trend of bilayer thickness, as illustrated by Fig. 2.

The film 100k40V exhibits a homogeneous nanocomposite structure composed of ~2 nm TiC nanocrystallites (NCs) embedded in C-rich amorphous matrix. By increasing the pulse frequency and thus the energy of ion impingement, the deposited atoms are able to diffuse over a larger depth, which facilitates local enrichment of Ti atoms and thus the subsequent formation of larger TiC NCs. These NCs align parallel to the surface, giving rise to a multilayered structure. In the film 250k40V, each Ti-rich sublayer contains one monolayer of TiC NCs of 3–5 nm diameter. The size of TiC NCs increases to 4–6 nm with p-dc frequency increasing to

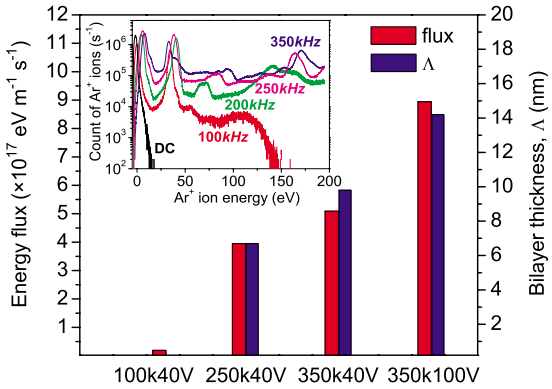

FIG. 2. (Color online) Diagram showing the trend of energy flux and bilayer thickness (except 100k40V where no layers form) at different deposition parameters with the inset showing the energy distribution of impinging ions at various p-dc frequencies.

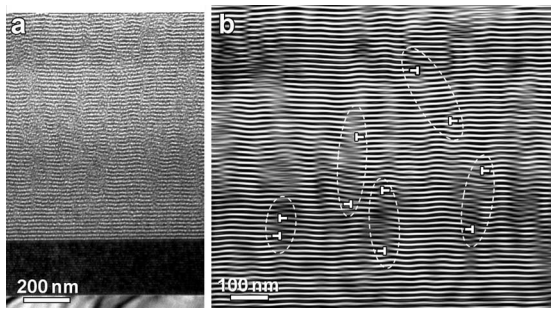

FIG. 3. (a) XTEM images showing the evolution of multilayers with growing thickness in the film 350k100V, (b) filtered inverse FFT image highlighting multilayer waviness with the maximum fluctuation smaller than a period, analogs to edge dislocations induced distortion in lattice planes in a crystal.

350 kHz. The further intensified ion impingement by applying higher bias voltage of 100V produces a stack of NCs in an individual Ti-rich layer in the film 350k100V, in addition to the larger wavelength. At the same time the size of the nanocrystallites is getting more scattered in a range of 3–7 nm. It is also noticed that in the films 250k40V and 350k40V the C-on-Ti and Ti-on-C interfaces show equally well defined contrast. However, in the 350k100V film, the Ti-on-C interface appears rather sharp, but the C-on-Ti interface appears relatively diffuse. The diffuseness is related to the random nucleation and growth of new (secondary) NCs that stack on the preformed (primary) NCs.

In contrast to the multilayers deposited layer by layer, whose waviness is governed by the surface roughness, the waviness of the multilayers presenting the self-organized distribution of TiC NCs is decoupled from the surface roughness and is more complex. In fact, this is also one of the major difficulties in maintaining the growth stability of the self-organized multilayers, in comparison with the modulation reported in literature that was generally lost after tens of nanometers growth. The XTEM micrograph in Fig. 3(a) shows the overall evolution of the multilayered structure of the film 350k100V. The waviness increases slightly at the early stage (approximately ten periods) but subsequently becomes saturated and stable. It is concluded that the intensive ion impingement used results in a continuously low or even decreasing roughness of the growing surface with deposition time, which ensures the self-assemble process and multilayered structure throughout the entire thickness of the films.

The waviness of the nanocomposite multilayers is highlighted in Fig. 3(b) by an inverse filtered fast Fourier transform treatment. Interestingly, the fluctuation of the multilayers, if deemed as crystallographical planes, resembles the distortion induced by edge dislocations. These "dislocation-like" defects introduce locally an extra layer of TiC NCs, resulting in distortion of the multilayers. The "dislocations" generally occur as dipoles, i.e., two dislocations with deferent signs close to each other locating at a vertical sliding plane. They cancel the effect of each other, and as a result, the fluctuation initiated at the lower "dislocation" is flattened out by the upper one. The "dislocation-glide-plane" in-between the two dislocations appears as a stripelike region with a locally diffuse appearance. HRTEM examination of the stripelike regions (not shown) reveals that the diffuse multilayered configuration is related to a local disorder of TiC NCs, i.e., imperfections in the self-organization.

A detailed HRTEM examination of the growing front discloses a very thin (~3 nm) capping layer or surface layer, which is invariably amorphous and covers the film. It is noticed that for a multilayered film the surface layer may contain alternating C-rich and Ti-rich segments as confirmed by the energy filtering TEM in Fig. 4(a), while the C-rich domains are not clearly distinguishable from the underneath a-C sublayer. However, this surface layer could be clearly observed in the film 350k40V0.55 shown in Fig. 4(c), which is composed of monolithic structure of TiC nanograins and a-C boundaries due to the largely increased Ti content. The existence and amorphous nature of the surface layer are mainly attributed to the greatly intensified concurrent impingement by p-dc sputtering at high frequencies. It is also a direct evidence of impingement induced subplantation model for surface smoothing in diamondlike carbon.[9] The surface layer was supposed to be sp^2 bonded carbon of a relatively low density,[9,10] but could not be imaged in pure a-C due to the lack of contrast.

The wavelength that can be tuned via the p-dc sputtering process is associated with an enhanced interdiffusion of C and Ti species caused by the concurrent ion impingement, a phenomenon noticed as early as in 1970–80s.[11,12] It was suggested that the high density of defects may be responsible for the enhanced diffusivity under intensified ion impingement. The impingement-enhanced diffusion coefficient $D^*(z)$ decays exponentially with depth z and can be expressed as[12]

$$D^*(z) = D^*(0)\exp\left(\frac{-z}{L_d}\right), \tag{1}$$

where $D^*(0)$ is the enhanced diffusion coefficient at the surface ($z=0$), and L_d represents a characteristic diffusion length of the ion-impingement-produced defects and can be assumed here as the wavelength Λ. For the present case, $D^*(0)$ is associated with the experimentally measured energy flux $\boldsymbol{I}$ illustrated in Fig. 2 and can be tentatively expressed in the form of

$$D^*(0) = D_{\text{th}}\exp\left(\frac{\alpha I}{kT}\right) = D_0\exp\left(-\frac{Q-\alpha I}{kT}\right), \tag{2}$$

with D_{th} representing the thermal diffusion coefficient of the phase separation given by the pre-exponential factor D_0 and the activation energy Q, $\exp(\alpha I/kT)$ being an enhancement factor and α is a positive constant. Equation (2) can be interpreted as an effective coefficient of thermal diffusion with the activation energy decreasing to $(Q\text{-}\alpha I)$ linearly with the energy flux. Therefore, Eqs. (1) and (2) provide a correlation between the bilayer thickness and the intensity of ion impingement as shown in Fig. 2.

The spatial coordinate z in Eq. (1) is related to the deposition rate v and deposition time t by $z=vt$. For a rough estimate, the diffusion length can be approximated by $L_d = 2\sqrt{\bar{D}^* t_\Lambda}$, where t_Λ is the deposition time for one bilayer and $\bar{D}^*$ the average impingement-enhanced interdiffusivity. By assuming the bilayer thickness as a measure of L_d, $\bar{D}^*$ is calculated for the films as listed in Table I, and the minus sign represents the up-hill nature of the interdiffusion.

The C-rich and Ti-rich segments in the surface layer indicate that the local composition of the layer is markedly influenced by the underneath wavy sublayers via the vertical diffusion process. For example, on the right side of Fig. 4(a) the capping layer is C-rich since the Ti atoms could travel a short distance downwards to the underneath Ti-rich layer. However, on the left side Ti atoms could not travel to the underneath Ti-rich layer due to the larger distance, consequently Ti is locally enriched and a new TiC nucleus marked by a circle forms at the bottom of the amorphous capping layer. This process initiates the formation of a new Ti-rich sublayer. While the capping layer is "flat," the waviness of the multilayers is thus restricted by the diffusion length. Once the amplitude of local waviness of the Ti-rich layer underneath the capping layer is larger than the diffusion length, an extra layer (dislocation) is introduced, causing local disordered arrangement of TiC NCs.

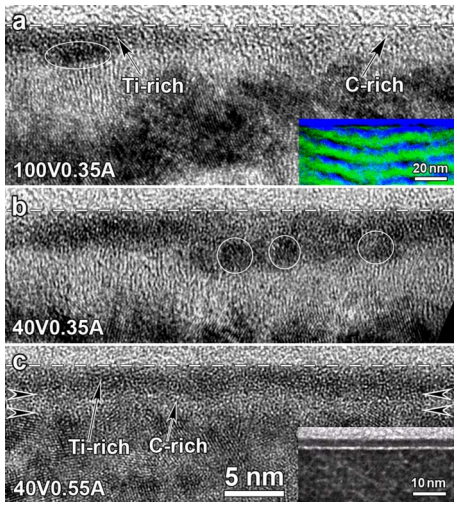

FIG. 4. (Color online) HR-XTEM of the growing front of films deposited at 350 kHz frequency, with the current to Ti target and substrate bias voltage indicated. A dashed line indicates the surface of the films. Insets are energy filtered compositional map [Ti green (light), C blue (dark)] at the growing front (a) and zoom out (c), respectively.

One final point to be considered is the driving force of phases separation, i.e., nucleation and growth versus spinodal decomposition. The wide size distribution of TiC NCs and especially the fine TiC NCs formed right at the bottom of the amorphous capping layer [Figs. 4(a) and 4(b)] indicate nucleation and growth mechanism.

[1]I. Daruka and J. Tersoff, Phys. Rev. Lett. **95**, 076102 (2005).
[2]J. H. He, C. A. Carosella, G. K. Hubler, S. B. Qadri, and J. A. Sprague, Phys. Rev. Lett. **96**, 056105 (2006).
[3]W. Y. Wu and Y. M. Ting, Chem. Phys. Lett. **388**, 312 (2004).
[4]I. Gerhards, H. Stillrich, C. Ronning, H. Hofsäss, and M. Seibt, Phys. Rev. B **70**, 245418 (2004).
[5]C. Corbella, B. Echebarria, L. Ramírez-Piscina, E. Pascual, J. L. Andújar, and E. Bertran, Appl. Phys. Lett. **87**, 213117 (2005).
[6]P. E. Hovsepian, Y. N. Kok, A. P. Ehiasarian, R. Haasch, J. G. Wen, and I. Petrov, Surf. Coat. Technol. **200**, 1572 (2005).
[7]G. Abrasonis, G. J. Kovács, L. Ryves, M. Krause, A. Mücklich, F. Munnik, T. W. H. Oates, M. M. M. Bilek, and W. Möller, J. Appl. Phys. **105**, 083518 (2009).
[8]Y. T. Pei, C. Q. Chen, K. P. Shaha, J. Th. M. De Hosson, J. W. Bradley, S. A. Voronin, and M. Cada, Acta Mater. **56**, 696 (2008).
[9]M. Moseler, P. Gumbsch, C. Casiraghi, A. C. Ferrari, and J. Robertson, Science **309**, 1545 (2005).
[10]C. A. Davis, G. A. J. Amaratunga, and K. M. Knowles, Phys. Rev. Lett. **80**, 3280 (1998).
[11]R. L. Minear, D. G. Nelson, and J. F. Gibbons, J. Appl. Phys. **43**, 3468 (1972).
[12]A. H. Eltoukhy and J. E. Greene, Appl. Phys. Lett. **33**, 343 (1978).